Science of the Total Environment 568 (2016) 285–295

Contents lists available at ScienceDirect

Science of the Total Environment

journal homepage: www.elsevier.com/locate/scitotenv

Atmospheric dry deposition of sulfur and nitrogen in the Athabasca Oil Sands Region, Alberta, Canada

Yu-Mei Hsu [a,*], Andrzej Bytnerowicz [b], Mark E. Fenn [b], Kevin E. Percy [a]

[a] Wood Buffalo Environmental Association, #100-330 Thickwood Blvd., Fort McMurray, Alberta T9K 1Y1, Canada
[b] US Department of Agriculture, Forest Service, Pacific Southwest Research Station, 4955 Canyon Crest Dr., Riverside, CA 92507, USA

HIGHLIGHTS

- NH_3, HNO_3, NO_2, and SO_2 concentrations were characterized by passive measurements.
- Dry deposition fluxes of N and S were estimated by a multi-layer model.
- Spatial distributions of N and S dry deposition in the AOSR were determined.

GRAPHICAL ABSTRACT

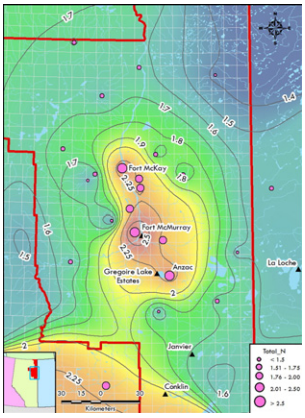

ARTICLE INFO

Article history:
Received 1 April 2016
Received in revised form 27 May 2016
Accepted 29 May 2016
Available online 10 June 2016

Editor: Elena PAOLETTI

Keywords:
Passive samplers
Atmospheric dry deposition
Nitrogen
Sulfur
Multi-layer inference model
Throughfall measurement

ABSTRACT

Due to the potential ecological effects on terrestrial and aquatic ecosystems from atmospheric deposition in the Athabasca Oil Sands Region (AOSR), Alberta, Canada, this study was implemented to estimate atmospheric nitrogen (N) and sulfur (S) inputs. Passive samplers were used to measure ambient concentrations of ammonia (NH_3), nitrogen dioxide (NO_2), nitric acid/nitrous acid (HNO_3/HONO), and sulfur dioxide (SO_2) in the AOSR. Concentrations of NO_2 and SO_2 in winter were higher than those in summer, while seasonal differences of NH_3 and HNO_3/HONO showed an opposite trend, with higher values in summer. Concentrations of NH_3, NO_2 and SO_2 were high close to the emission sources (oil sands operations and urban areas). NH_3 concentrations were also elevated in the southern portion of the domain indicating possible agricultural and urban emission sources to the southwest. HNO_3, an oxidation endpoint, showed wider ranges of concentrations and a larger spatial extent. Concentrations of NH_3, NO_2, HNO_3/HONO and SO_2 from passive measurements and their monthly deposition velocities calculated by a multi-layer inference model (MLM) were used to calculate dry deposition of N and S. NH_3 contributed the largest fraction of deposited N across the network, ranging between 0.70–1.25 kg N ha^{-1} yr^{-1}, HNO_3/HONO deposition ranged between 0.30–0.90 kg N ha^{-1} yr^{-1}, and NO_2 deposition between 0.03–0.70 kg N ha^{-1} yr^{-1}. During the modeled period, average dry deposition of the inorganic gaseous N species ranged between 1.03 and 2.85 kg N ha^{-1} yr^{-1} and SO_4-S deposition ranged between 0.26 and 2.04 kg ha^{-1} yr^{-1}. Comparisons with co-measured ion exchange resin throughfall data (8.51 kg S ha^{-1} yr^{-1}) indicate that modeled dry deposition

* Corresponding author.
E-mail address: yhsu@wbea.org (Y.-M. Hsu).

http://dx.doi.org/10.1016/j.scitotenv.2016.05.205

combined with measured wet deposition (1.37 kg S ha^{-1} yr^{-1}) underestimated S deposition. Gas phase NH_3 (71%) and HNO_3 plus NO_2 (79%) dry deposition fluxes dominated the total deposition of NH_4-N and NO_3-N, respectively.

1. Introduction

Oil sands are a mixture of clay, sand, water and crude bitumen containing heavy molecular weight hydrocarbons used for production of asphalt, oil and various petroleum derivatives. Canada's Oil Sands in the Athabasca, Peace River and Cold Lake regions of Alberta, cover some 140,200 km^2 (Alberta Energy, 2011). Large-scale oil bitumen exploitation and processing in the Athabasca Oil Sands Region (AOSR) in northeastern Alberta has raised environmental concerns, partially due to the potential for eutrophication of terrestrial and aquatic ecosystems (Aherne and Shaw, 2010). In the AOSR, there are various emission sources including natural (e.g. forest fires and vegetation), oil sands operations (i.e. fixed, mobile, fugitive), and urban/transportation. Nitrogen oxide (NO_x), sulfur dioxide (SO_2), carbon monoxide and volatile organic compounds are the major criteria air contaminants emitted from the oil sands processes. According to the Canadian National Pollutant Release Inventory (NPRI), 2013 stack emissions of ammonia (NH_3), nitrogen oxides (NO_x) and SO_2 in the region were 4.4, 102 and 238 t d^{-1}, respectively (http://www.ec.gc.ca/inrp-npri/). However, NH_3 emissions may be underestimated in these inventories (Fenn et al., 2015). Facility reporting indicates stacks (main, flue-gas desulfurization) as the major SO_2 sources with NO_x emission sources being split between stacks and area sources (i.e. mine-fleets) at ratios dependent upon process used.

Nitrogen dioxide is produced during oxidation of NO emitted during combustion processes, including fossil fuel combustion, forest fires, and other natural and anthropogenic processes (Finlayson-Pitts and Pitts, 2000). Nitric acid (HNO_3) is a final product of complex photochemical reactions between NO, NO_2, O· and OH·. NH_3 emissions result from agricultural activities, biological decay processes, catalytic converters, smoldering phase of fires, from flue gas desulfurization systems (Wang et al., 2012). NH_3, NO_2 and HNO_3 are important components of reactive atmospheric nitrogen (N_r) and major drivers of atmospheric nitrogen (N) dry deposition to forests and other ecosystems (Bytnerowicz and Fenn, 1996; Hanson and Lindberg, 1991). Sulfur dioxide may be released during natural processes (e.g., volcanic emissions) and from anthropogenic activities such as combustion of fossil fuels, refining and smelting of sulfide ores, and other industrial processes (Seinfeld and Pandis, 2006). Through stomatal uptake, it is an important source of S deposition to vegetation including forest ecosystems (Fowler et al., 1989).

The Wood Buffalo Environmental Association (WBEA; www.wbea.org) is a multi-stakeholder, not-for-profit organization responsible for monitoring air quality in the AOSR. Outside of the Athabasca River Valley in the boreal forest, WBEA has used passive sampling techniques since 2000 to measure ambient concentrations of selected air pollutants for providing estimates of air pollutant exposure to forests and other vegetation. Passive samplers are simple to use, inexpensive, do not require electricity or air conditioned shelters and thus can be used in remote locations (Bytnerowicz et al., 2005; Krupa and Legge, 2000). As such, passive samplers allow for a spatial coverage of the areas of interest providing data that can be used for the generation of geostatistical maps of air pollutants. The information gathered helps to better understand atmospheric composition and distribution of air pollutants, atmospheric dry deposition of N (NH_3, HNO_3, and NO_2) and S (SO_2), as well as regional imports and exports.

In this study, ambient concentrations of selected inorganic N and S gaseous species and their dry deposition amounts have been determined to elicit an improved understanding of potential effects of gaseous phase N and S on the terrestrial ecosystems of the AOSR.

2. Methods

2.1. Monitoring network

WBEA operates a regional monitoring program focused in part on assessing whether or not emissions of acidifying and eutrophyting compounds are having adverse effects on the terrestrial environment in the AOSR. This program is well described in Percy (2013). A passive sampler network was established in the region to characterize the spatial distribution of pollutants and their deposition by using geostatistical methods. Coordinates and a detailed map of all AOSR monitoring sites, including those for the ion exchange resin (IER) deposition determinations is also shown in Supplementary information (SI) Table S1 and Fig. S1.

2.2. NH_3, HNO_3/HONO, NO_2 and SO_2 passive measurements

Passive samplers to monitor NH_3, HNO_3 with nitrous acid (HONO), NO_2 and SO_2 were exposed to ambient air on towers above the tree canopy or on posts at a height of 2 m above ground level in the industrial areas of the AOSR and at 2 m above bog surfaces. Passive samplers were collected every month in summer (from April to September) and every two months in winter (from October to March). Ambient NH_3 and HNO_3/HONO concentrations were monitored near the mining and industrial operations and in remote areas of the AOSR from 2005 until 2013. The monitoring network for NH_3 and HNO_3/HONO consisted of 25 sites in 2005, gradually grew to 38 sites in 2009 and was reduced to 26 sites for 2010–2013. The passive sampling program for NO_2 and SO_2 concentrations have been initiated in 1999 at 11 sites, gradually increased to 15 sites in 2005 and to 23 sites in August 2008.

Passive samplers of the Ogawa design (Ogawa & Co. USA, Inc.) (Roadman et al., 2003) were used for NH_3 monitoring with two replicate filters coated with citric acid. Three replicate HNO_3/HONO samplers of the US Department of Agriculture Forest Service (USDA FS) design (Bytnerowicz et al., 2016; Bytnerowicz et al., 2005) were used at each monitoring site. In these samplers, ambient air passes through a Teflon membrane and both HNO_3 and HONO species are absorbed on a Nylasorb nylon filter as nitrate (NO_3^-). After sampling, exposed samplers of HNO_3/HONO and NH_3 were shipped to the USDA FS chemical laboratory in Riverside, California for sample analysis. Both NH_3 and HNO_3/HONO samples were extracted by de-ionized (DI) water and analyzed using a TRAACS 2000 autoanalyzer for ammonium (NH_4^+) and an ion chromatography system (ICS, Dionex ICS 2000 LCD, Dionex Corp., now Thermo Fisher Scientific Inc.) for NO_3^-. Ambient NH_3 and HNO_3/HONO concentrations were calculated based on a comparison of passive samplers against the collocated honeycomb denuder systems (Koutrakis et al., 1993). In field trials performed in Riverside, California, the samplers showed high accuracy (relative standard deviation of three replicate readings of ~5%)(Bytnerowicz et al., 2010).

The all-season SO_2 passive sampling system (SPSS) (Tang et al., 1997), and NO_2 passive sampling system (NPSS) (Tang et al., 1999) were installed at the network locations to estimate SO_2 and NO_2 concentrations, respectively (Hsu, 2013). After collection, SO_2 and NO_2 samples were extracted in DI water and analyzed by an ICS (DX-120,

Dionex Corp., now Thermo Fisher Scientific Inc.) for sulfate (SO_4^{2-}) and nitrite (NO_2^-) concentrations by Maxxam Analytic Inc.

2.3. Estimating dry deposition flux using the multi-layer inferential model

The National Oceanic and Atmospheric Administration (NOAA) multilayer inferential model (MLM) was used to estimate dry deposition flux for NH_3, HNO_3, NO_2, and SO_2 at 23 sites (SI Table S1). A brief description of MLM and how it has been used is provided below. A more complete description of the methods could be found in Meyers et al. (1998) and Cooter and Schwede (2000).

Dry deposition velocity (V_d) of chemical species of interest is estimated by MLM applying an inference approach which assumes that dry deposition flux (F) is the linear product of ambient concentration of chemical species (C) at some reference height and chemical species deposition velocity (V_d) (Meyers et al., 1998; Wesely and Hicks, 2000):

$$F = C \times V_d \quad (1)$$

The MLM is based on a resistance model framework analogous to Ohm's Law (Meyers et al., 1998):

$$V_d = 1/(R_a + R_c) \quad (2)$$

Where R_a = aerodynamic resistance between some height (a shallow sub-layer within the atmospheric constant flux layer, as a function of atmospheric turbulence and stability, and surface characteristics) above local ground and the canopy height, and R_c = total canopy resistance. Equations for R_a and R_c calculation have been described in Meyers et al. (1998).

The deposition velocity values used by the MLM model in this study were calculated by applying environmental parameters from each site, including leaf area index, temperature, humidity, wind speed, standard deviation of wind direction and solar radiation. Thus, the deposition velocity values derived in this study are site specific. In the AOSR, the major overstory plants are jack pine (*Pinus banksiana* Lamb.) and aspen (*Populus tremuloides* Michx.) and the major ground cover plant is the reindeer lichen (*Cladina mitis* Sandst.). Plant cover types and percent of foliage for the major plant type observed at each site were used to estimate leaf area index.

For mapping, ArcGIS (ESRI) with Kriging was used to generate isopleth maps for the annual average deposition for NH_3-N, HNO_3-N, NO_2-N, total N, and SO_2-S.

2.4. Meteorological measurements

Meteorological data used by MLM were collected hourly at four of WBEA's community air monitoring stations (AMS), including AMS 1 (Bertha Granter-Fort McKay) located in Fort McKay, AMS 6 (Patricia McInnes) and AMS 7 (Athabasca Valley) in Fort McMurray, and AMS 14 (Anzac) in Anzac. The meteorological measurements included temperature, standard deviation of wind speed, wind direction, relative humidity and solar radiation. All data and methods including detailed standard operating and QA/QC procedures are available at www.wbea.org.

2.5. Wet precipitation and $PM_{2.5}$ measurements

Wet precipitation was collected on a weekly basis by a wet-only precipitation collector (Meteorological Instruments of Canada corp.) located in an open site (AMS 1) and analyzed by IC for SO_4^{2-}, NO_3^-, NH_4^+ concentrations. For $PM_{2.5}$ (particulate matter with an aerodynamic diameter smaller than 2.5 μm), 24-hour $PM_{2.5}$ samples were collected by an US Federal Reference Method Partisol $PM_{2.5}$ sampler once every six days (following the schedule of the Canadian National Air Pollution Surveillance Program, http://www.ec.gc.ca/rnspa-naps/). After sampling, samples were extracted by DI water and analyzed by IC for both cation and anion. For both measurements, the standard operation procedures and QA/QC processes could be found at www.wbea.org.

2.6. Ion exchange resin measurement

The ion exchange resin (IER) technique has been employed in the AOSR for measuring atmospheric deposition (including bulk deposition in open sites and throughfall under tree canopies) of N and S species in the AOSR since May 2008 (Fenn et al., 2015; Fenn and Poth, 2004; Fenn et al., 2013). With IER collectors, ions in solution are retained on the ion exchange resin columns during the field exposure and later extracted in the laboratory for calculation of deposition fluxes. Throughfall or bulk deposition fluxes measured with IER samplers is equivalent to fluxes measured with conventional solution samplers (Fenn and Poth, 2004). Throughfall samples include both wet deposition and wet-scavenged dry gaseous and particulate deposition washed from the canopy (Fenn and Poth, 2004). In contrast, collectors located in open areas (IER open samples) collect primarily wet deposition (Fenn et al., 2015) along with some residual dry deposition deposited to the collector surface during dry periods. The IER samplers were deployed for six months for two seasons each year: summer from May to October and winter from November to April.

In summary, three kinds of empirical deposition measurements were employed in this study: (1) wet deposition from wet-only precipitation measurements, (2) bulk deposition measurements with IER samplers located in open, canopy-free sites (samples are mainly wet deposition with some dry deposition to the collectors during dry periods, and (3) bulk throughfall measurements with IER samplers located under jack pine canopies. Throughfall N deposition for example, can be considered as wet + dry N deposition to the canopy minus any canopy N retention (Fenn et al., 2013). Comparisons of N and S deposition in bulk deposition and in throughfall with wet deposition plus MLM-estimated dry deposition was conducted at AMS 1 where data on the concentrations of ionic species for wet precipitation and the particulate phase (http://www.wbea.org/monitoring-stations-and-data/integrated-data) are available from the direct measurements described in Section 2.5.

2.7. Statistical analysis

Non-parametric statistical analyses were employed for this study, including: (1) Mann-Whitney rank sum test (Sigmaplot® 11, San Jose, CA, USA) for data comparison; (2) Spearman rank order correlation (SigmaPlot® 11) for correlation coefficient analysis.

3. Results and discussion

3.1. Ambient concentrations from passive measurements

3.1.1. Ammonia

Between May 2005 and September 2013, NH_3 concentrations (ambient condition for temperature and pressure) in the summer months (1.96 ± 0.83 μg m^{-3}) at all sites were higher than those in the winter months (1.10 ± 0.53 μg m^{-3}). Peak NH_3 values approached 25 μg m^{-3} during summer 2011, although most values were generally <10 μg m^{-3} (Fig. 1a). The annual average concentrations at all 23 sites ranged from 1.29 μg m^{-3} in 2010 to 2.01 μg m^{-3} in 2012. Ammonia had the highest values in the centre of the AOSR operations, and in the S and SW portions of the study domain (Bytnerowicz et al., 2010; Hsu and Bytnerowicz, 2015). Elevated NH_3 concentrations in the S and SW portion of the monitored area in summer could be caused by long-range transport of the pollutant from the agricultural areas of Edmonton, Athabasca and the surrounding areas, aided by the winds from the SW and S. In conditions of low relative humidity, NH_3 can be transported long-distance from

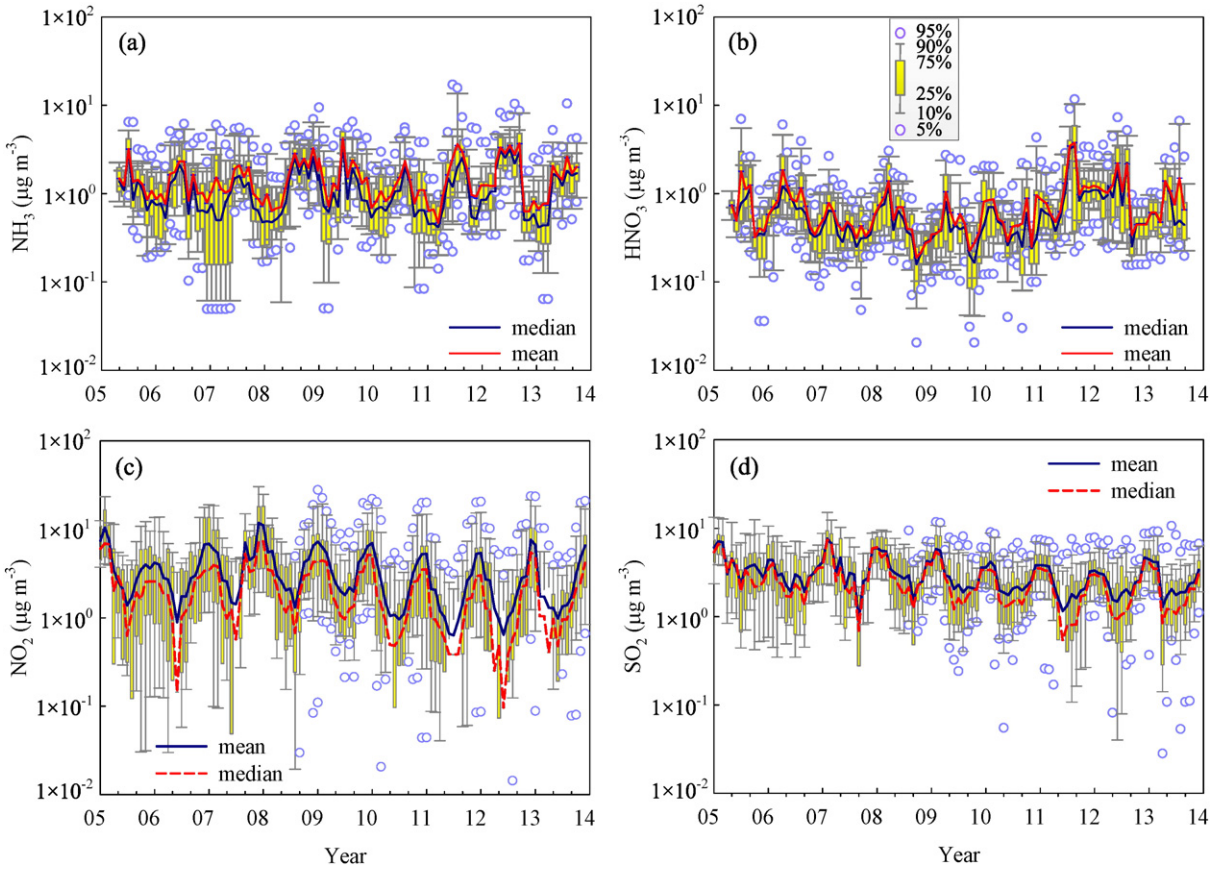

Fig. 1. Monthly concentrations (μg m^{-3}) from passive measurements across the air monitoring network in the AOSR from 2005 to 2013 for (a) NH_3, (b) HNO_3/HONO, (c) NO_2 and (d) SO_2.

the pollution-source areas as has been shown for the eastern parts of the Sierra Nevada affected by agricultural emissions from the Central Valley of California (Bytnerowicz et al., 2014). This phenomenon was not observed during winter in the absence of agricultural activities, and the highest NH_3 values were limited to the industrial center of the AOSR. The highest values that occurred in summer 2011 were most likely caused by extensive forest fires in the AOSR during that period (Percy et al., 2012).

3.1.2. Nitric acid/nitrous acid

From May 2005 until September 2013, HNO_3/HONO concentrations were quite variable (Fig. 1b) and the annual average concentrations at all 23 sites ranged from 0.48 μg m^{-3} in 2007 to 1.37 μg m^{-3} in 2011. Concentrations of this secondary pollutant in winter (0.67 ± 0.33 μg m^{-3}) were slightly lower than in summer (0.88 ± 0.73 μg m^{-3}) which is consistent with earlier observations (Bytnerowicz et al., 2010; Hsu and Clair, 2015). In summer, HNO_3/HONO concentrations were higher due to the photochemical nature of this pollutant in the region (Hsu and Clair, 2015). The highest values approaching 12 μg m^{-3} were measured during the 2011 summer season. It should be emphasized that the observed elevated HNO_3/HONO concentrations in summer 2011 were most likely caused by extensive forest fires in the AOSR during that period. Two potential mechanisms could be envisioned: (1) reduction of NO_2 emitted from fires to nitrous acid on soot aerosol particles (Kalberer et al., 1999) and its subsequent oxidation to HNO_3, and (2) photochemical HNO_3 formation fed by high concentrations of NO_x and VOCs (volatile organic compounds) emitted from fires (Seinfeld and Pandis, 2006). During the period, the highest HNO_3/HONO concentrations were found both in the center of the AOSR and further away to the NE, far away of the AOSR industrial activities (Hsu and Bytnerowicz, 2015).

3.1.3. Nitrogen dioxide

Monthly NO_2 concentrations from January 2005 to December 2013 (Fig. 1c) showed a strong seasonal pattern. Concentrations were high in winter (4.59 ± 5.26 μg m^{-3}) and low in summer (1.94 ± 2.26 μg m^{-3}). The annual average NO_2 concentrations at all 23 sites ranged from 2.21 μg m^{-3} in 2011 to 4.77 μg m^{-3} in 2007. For the spatial variation, elevated NO_2 concentrations were observed near the major industrial emissions and residential areas in Fort McMurray in both winter (Fig. 2a) and summer (Fig. 2b). In the summer, the higher NO_2 concentrations were more localized, and limited to a small area close to the major emission sources. In winter, the elevated NO_2 concentrations were distributed more widely, particularly to the north due to the influence of the Athabasca Valley which enhances the flow of winds moving from south to north as shown in Fig. 2a.

Nitrogen oxides are primary pollutants emitted from sources in the AOSR undergo atmospheric chemical reactions to form secondary pollutants and contribute to dry deposition. The ambient NO_2 concentrations in this study were mainly controlled by emission rates and meteorological conditions in the AOSR. In the winter months, higher NO_x emissions resulted from more NO_x emitted from oil sands mining process boilers and heaters as steam requirements to process the colder temperature mined bitumen and also from both the on-road and non-road vehicles and heating (e.g., residential houses and industries). Furthermore, the meteorological conditions in winter (e.g., low temperature, stable atmosphere, less sunlight, low mixing height) did not favor optimum NO_x dilution, NO_x photochemical reactions, or

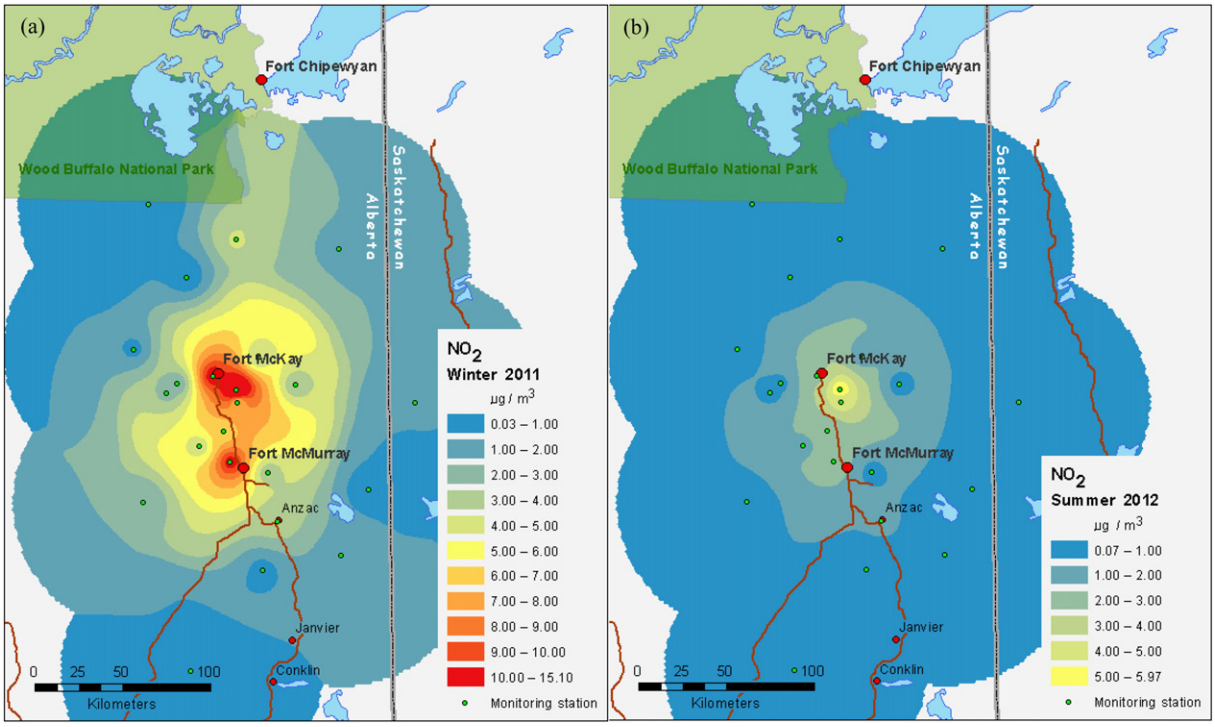

Fig. 2. Spatial variation of NO_2 concentrations for (a) winter 2011 and (b) summer 2012.

atmospheric deposition of NO and NO_2. These factors resulted in longer atmospheric residence times of NO_2 in the winter months (Hsu and Bytnerowicz, 2015).

3.1.4. Sulfur dioxide

The annual average SO_2 concentrations at all sites ranged from 2.48 μg m^{-3} in 2011 to 4.23 μg m^{-3} in 2005. Monthly SO_2 concentrations from 2005 to 2013 in the AOSR are displayed in Fig. 1d. The SO_2 concentrations had a seasonal pattern: low values in summer (2.19 ± 1.87 μg m^{-3}) and high values in winter (3.75 ± 2.27 μg m^{-3}). The lower mixing height and stable atmosphere are probably the major reasons for the relatively high SO_2 concentrations in the winter months (Hsu, 2013). SO_2 concentrations were lower in summer since (1) SO_2 in the ambient air could be diluted more quickly, and (2) SO_2 reactions including dry deposition and heterogeneous reactions with aerosols (Seinfeld and Pandis, 2006), are usually faster in summer due to

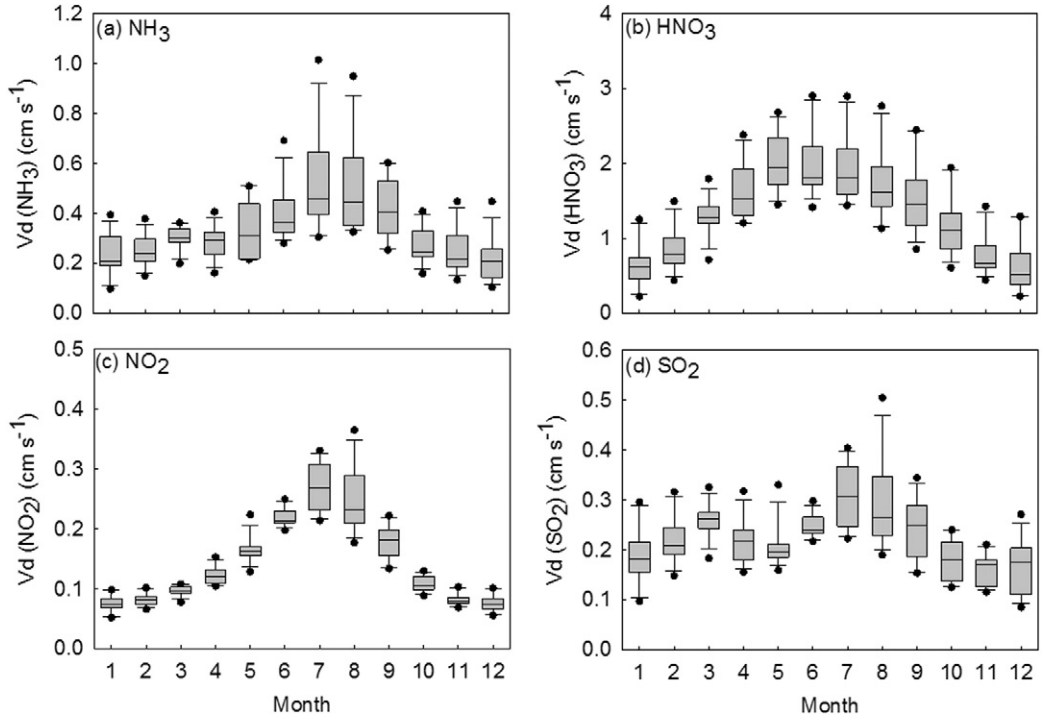

Fig. 3. Monthly deposition velocities for (a) NH_3, (b) HNO_3, (c) NO_2 and (d) SO_2 at AMS 1 (from 2005 to 2012) calculated by MLM (AMS: air monitoring station; MLM: multilayer inferential model).

increased exposure to moist surfaces, higher concentrations of oxidants, and higher temperatures.

Elevated SO_2 concentrations were observed near the major industrial emissions, e.g., stacks. After release from the emission sources, SO_2 undergoes dilution, chemical reaction and deposition, resulting in rapidly decreasing concentrations. The spatial distribution of SO_2 concentration is localized and limited to a small area close to the upgrading emission sources in summer months as well.

3.2. Nitrogen and sulfur dry deposition estimates based on passive sampler data

In North America, two models (MLM and Big Leaf Model [BLM]) have been used by long-term monitoring networks (including CASTNet and CAPMoN) to calculate the V_d and dry deposition flux. In the AOSR, the major overstory plants are jack pine and aspen and the major ground cover plant is reindeer moss (lichen). Monthly deposition velocities (V_d) were calculated by the MLM for NH_3, HNO_3, NO_2 and SO_2 from 2005 to 2012 at AMS 1 and their values were generally higher in summer than in winter (Fig. 3). The maximum V_d occurred in July for both NH_3 and NO_2; in May, June and July for HNO_3; and in March and July for SO_2; the smallest V_d values for four species were observed in winter. Since V_d for NH_3, HNO_3, NO_2 and SO_2 is influenced by both the ground and vegetation cover and aerodynamic resistance, higher V_d in March and April (snow melting) reflects the more exposed canopy (due to loss of snow cover) and standing water (or moist) ground cover with the combination of higher wind speeds. The V_d reaches the highest values in summer months because of more foliated forest canopies and water ground available for deposition. Estimated V_d values of NH_3, NO_2 and HNO_3 are within a reasonable range compared to earlier studies in both MLM and BLM (Adon et al., 2013; Brook et al., 1999; Krupa, 2003; Schwede et al., 2011; Sickles and Shadwick, 2007a; Sickles and Shadwick, 2007b; Zhang et al., 2009). However, V_d (SO_2) calculated by MLM was lower than that by BLM (Schwede et al., 2011). It is unclear how accurate the models are or which is the best for SO_2 deposition at the AOSR. We used the MLM, taking this uncertainty into account. Further studies should be conducted to evaluate differences in dry deposition flux from the two models in the AOSR and to determine if MLM or BLM is better for the deposition estimation.

For this study, dry deposition of S (i.e., SO_2) and N (i.e., NH_3, HNO_3 and NO_2) was calculated from January 2006 to December 2012. In August 2008, the sampling sites for the SO_2 and NO_2 have been increased to 23 sites. For the consistency of sampling sites, the annual deposition results from 2009 to 2012 were used for the deposition mapping.

3.2.1. NH_3 dry deposition

Ammonia deposition values for 23 monitoring sites were calculated for individual years during the 2006–2012 period and showed values ranging from 0.36 kg N ha^{-1} yr^{-1} in 2007, to 2.35 kg N ha^{-1} yr^{-1} in 2011. A map of average annual distribution for the 2009–2012 period (Fig. 4a) shows two areas of high NH_3 deposition – one in the center of the AOSR between Anzac and Fort McKay; and the second larger area in the southern portion of the monitoring area. The first area reflects deposition caused by elevated NH_3 emissions and concentrations during oil exploitation and processing, including from local community activities, in the AOSR. The second area was most likely affected by long-range NH_3 transport from the Edmonton agglomeration as well as other urban and agricultural areas south of the AOSR. In general, the calculated 4-year average NH_3 deposition ranged between 0.59 to 1.33 kg N ha^{-1} yr^{-1}. These values were higher than the dry deposition values for HNO_3 or NO_2 (Sections 3.2.2 and 3.2.3) indicating that NH_3 was the major species contributing to N dry deposition as has been reported previously from throughfall and bulk deposition studies in the AOSR (Fenn et al., 2015).

3.2.2. HNO_3 dry deposition

Deposition of HNO_3 across the monitoring network during the 2006–2012 period ranged between 0.16 kg ha^{-1} yr^{-1} in 2007 and 1.94 kg ha^{-1} yr^{-1} in 2012. Similar to NH_3, the highest HNO_3 deposition values were determined in the central area of the AOSR, and in its

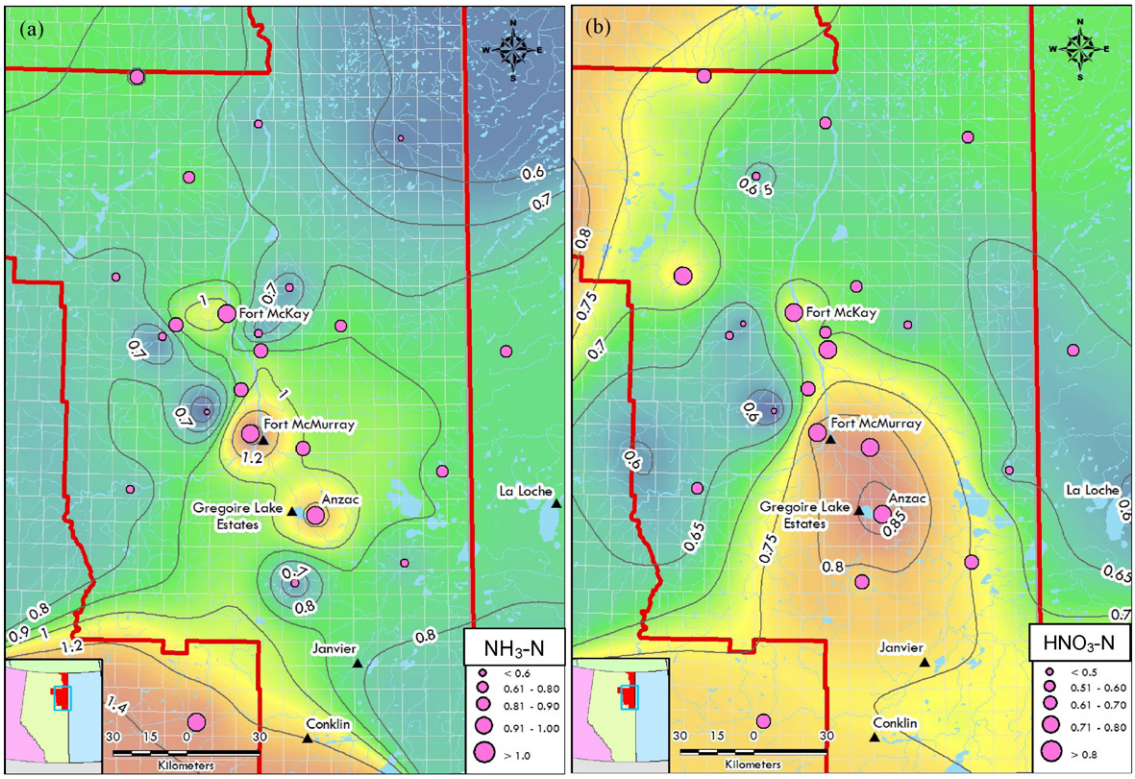

Fig. 4. Four-year annual average dry deposition from 2009 to 2012 in the AOSR in kg N ha^{-1} yr^{-1} for (a) NH_3-N; (b) HNO_3-N; (c) NO_2-N; (d) total N (N_r); and (e) SO_2-S (kg ha^{-1} yr^{-1}).

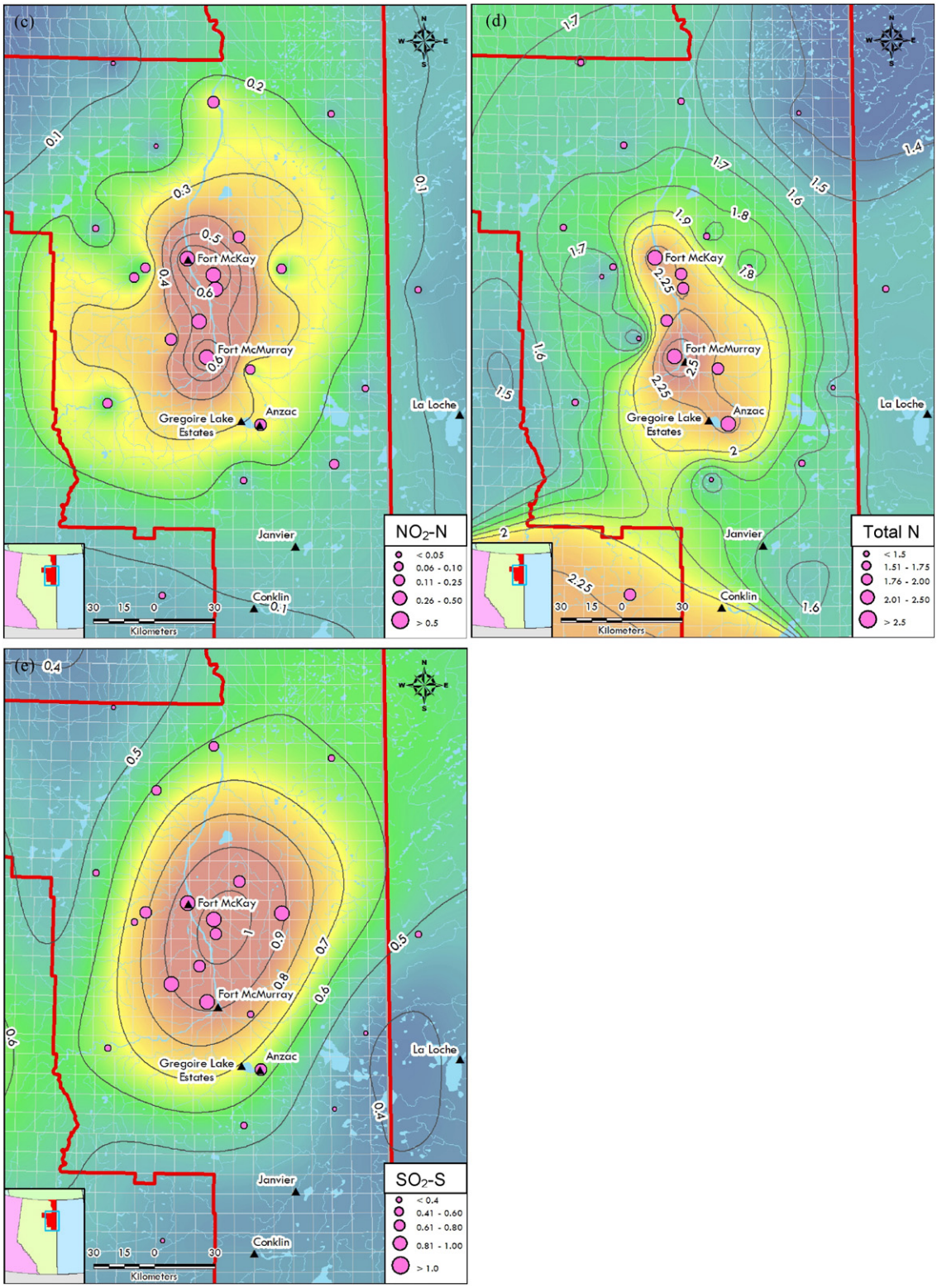

Fig. 4 (*continued*).

southern and northwestern portions (Fig. 4b). The elevated HNO_3 deposition in the northwest resulted from the 700,000 ha forest fire complex that occurred in 2011 (Bytnerowicz et al., 2016). Considering the high deposition velocity of HNO_3 (Fig. 3b), the spatial variation of HNO_3 deposition is essentially reflecting the spatial pattern of its concentrations. The 4-year average deposition values for this pollutant ranged between 0.33 and 1.24 kg N ha^{-1} yr^{-1}, and were slightly lower than the NH_3 deposition values. These values were in the similar range as those for the NO_2 deposition (Section 3.2.3, Fig. 4c).

3.2.3. NO_2 deposition

In winter, NO_2 concentrations were significantly higher than concentrations of HNO_3 and NH_3, resulting in NO_2 deposition being an important component for total N deposition in the AOSR. Nitrogen

dioxide dry deposition was estimated at 23 sites from 2009 to 2012 with the four-year annual average NO_2-N deposition ranging from 0.03 N ha^{-1} yr^{-1} in the northwestern area to 0.93 N ha^{-1} yr^{-1} in the central area of AOSR (Fig. 4c). After emission from the sources, NO_x undergoes dilution and photochemical reactions. The major NO_2 removal mechanism from the atmosphere is a photochemical reaction, reacting with OH radicals during the daytime and NO_3 radicals at night. The life time of NO_2 is around one day (Seinfeld and Pandis, 2006) during summer conditions in the AOSR. Because of this short life time, the major NO_2 deposition is localized relatively close to the emissions source area. The greatest NO_2 deposition (Fig. 4c) occurred in places where major oil sand operation activities occur, and where communities exist. Therefore, it may be assumed that elevated NO_2 deposition resulted from industrial emissions (e.g., stacks and mine fleets) at the sampling site near oil sands operation and from local community activities (e.g., on-road transportation) at sampling sites near a community.

3.2.4. Total dry deposition of reactive N

Total deposition of reactive inorganic gaseous N (N_r = $NH_3 + HNO_3 + NO_2$) across the network during the 2006–2012 period ranged between 0.70 kg N ha^{-1} yr^{-1} in 2010 to 4.15 kg N ha^{-1} yr^{-1} in 2006. A map of the average N_r sum distribution for the 2009–2012 period (Fig. 4d) shows two areas of high N deposition – one in the center of the AOSR between Anzac and Fort McKay with values reaching in Fort McMurray, and the second in the southern portion of the monitoring area with values approaching 2.0 kg N ha^{-1} yr^{-1}. Distribution patterns for total deposition of inorganic gaseous N are similar to those of the NH_3 deposition indicating relative importance of that pollutant as reported previously (Fenn et al., 2015). Nitric acid had a strong contribution to higher N deposition in the southern AOSR, while NO_2 contributed mainly to the elevated levels between Anzac and Fort McKay.

While higher deposition in the center of the AOSR is mainly related to the industrial emissions, the elevated deposition values in the southern part of the AOSR could be caused by agricultural activities in central Alberta as well as potential effects of forest fire emissions and long-range transport of pollutants.

3.2.5. SO_2 deposition

Sulfur dioxide in the ambient air is removed by dry and wet deposition, or is oxidized to sulfate. The SO_2 residence times are 60, 100 and 80 h based on removal by dry deposition, wet deposition and chemical reaction, respectively, and the overall residence time is 25 h when three mechanisms are combined (Seinfeld and Pandis, 2006). All three removal mechanisms are important for ambient SO_2 concentration. The SO_2-S dry deposition was calculated at 13 sites from 2006 to 2008 and 23 sites from 2009 to 2012. Annual averages ranged from 0.26 kg S ha^{-1} yr^{-1} in 2011 to 2.04 kg S ha^{-1} yr^{-1} in 2006. The lowest SO_2-S deposition was 0.26 kg ha^{-1} yr^{-1} at a site 80 km south of Fort McKay. The highest SO_2 deposition was observed near the major SO_2 emission sources, i.e., stacks (Fig. 4e). Based on Environment Canada's National Pollution Release Inventory (NPRI), there were three major SO_2 emitting facilities in the oil sands operation area with emissions from these facilities associated with stacks and the highest deposition occurred in the same area. Elevated SO_2 deposition was also observed in Fort McMurray, an urban transportation hub.

3.3. Comparison with IER throughfall flux

Throughfall samples include both wet deposition and dry deposition, although a portion of the atmospherically-deposited N is retained by the canopy(Fenn et al., 2013; Lovett and Lindberg, 1993). In contrast, for S deposition, throughfall fluxes are generally very similar to total S deposition fluxes (Butler and Likens, 1995; Lindberg and Lovett, 1992). For the comparison with IER throughfall deposition, two measures (MLM plus wet deposition, referred to as MLM/wet) should be employed for total NH_4-N, NO_3-N, and SO_4-S deposition flux calculation as shown in Eqs. (3)–(5). Calculated total NH_4-N flux, consists of wet deposition of NH_4-N, [wNH_4-N], from the direct measurement, and dry deposition calculated by the MLM for gaseous phase NH_3, [gNH_3-N], and particulate phase NH_4-N, [pNH_4-N].

$$\text{Flux}\ (NH_4\text{—N}) = [wNH_4\text{—N}] + [gNH_3\text{—N}] + [pNH_4\text{—N}] \quad (3)$$

The total NH_4-N deposition at AMS 1 from MLM/wet and IER are displayed in Fig. 5a, and the total NH_4-N deposition from two methods agreed well with a correlation coefficient (r) of 0.82 ($p = 0.01$). Both methods showed that the NH_4-N deposition in summer was higher than that in winter. Wet deposition of NH_4-N dominated the NH_4-N deposition in summer months, and gaseous phase NH_3 deposition was the dominant form regardless of seasons. The average dry deposition percentage of total deposition was 71%. The four-year annual average (2008–2011) was 0.86 kg N ha^{-1} yr^{-1} for total NH_4-N deposition from MLM/wet and 0.79 kg N ha^{-1} yr^{-1} from IER throughfall measurement. A non-parametric analysis (Mann-Whitney Rank Sum Test) shows there is no statistically significant difference between the MLM/wet and IER throughfall results ($p = 0.80$) or between the MLM/wet and IER open results ($p = 0.54$).

The total NO_3-N deposition flux at AMS1, Flux (NO_3-N), includes the dry deposition from gaseous phase NO_2, [gNO_2-N], and HNO_3, [gHNO_3-N], particulate phase NO_3^-, [pNO_3-N], and the wet deposition form NO_3^-, [wNO_3-N], as shown in Fig. 5b.

$$\text{Flux}\ (NO_3\text{—N}) = [gNO_2\text{—N}] + [gHNO_3\text{—N}] + [pNO_3\text{—N}] + [wNO_3\text{—N}] \quad (4)$$

The results from the MLM/wet were in the range of IER throughfall results ($p = 0.10$). However, the NO_3^- deposition trends from the two methods showed no significant relationship ($r = 0.20$, $p = 0.66$). The 2008–2011 annual average was 1.05 kg N ha^{-1} yr^{-1} for total NO_3-N deposition from MLM/wet and 0.44 kg N ha^{-1} yr^{-1} from IER throughfall measurement. The dry deposition was 79% of total deposition. The wet deposition contributed the NO_3-N deposition more significantly in summer months. For dry deposition, gas phase NO_2 and HNO_3 deposition dominated the NO_3-N deposition and NO_2 deposition flux in winter months were higher than that of HNO_3. This is due to the elevated NO_2 concentrations in winter in the AOSR, as described earlier. In the summer of 2011, forest fires burned within a few km of the sampling site (AMS 1) resulting in elevated concentrations of gas phase HNO_3 and particulate phase NO_3^-. As shown in Eq. (1), the deposition flux of a given atmospheric contaminant is in proportion to its ambient concentration. In summer 2011, the NO_3-N deposition flux increased as the concentrations increased for both gas phase HNO_3 and particulate phase NO_3^-.

The total SO_4-S deposition flux at AMS 1, Flux (SO_4-S), includes dry deposition of gaseous phase SO_2-S, [gSO_2-S], and particulate phase SO_4-S, [pSO_4-S], as well as wet deposition of SO_4-S, [wSO_4-S].

$$\text{Flux}\ (SO_4\text{—S}) = [gSO_2\text{—S}] + [pSO_4\text{—S}] + [wSO_4\text{—S}] \quad (5)$$

As shown in Fig. 5c, the wet deposition of SO_4-S was the major form for SO_4-S in summer months. The gaseous phase SO_2 was the dominant deposition form for dry SO_4-S deposition and the gaseous phase SO_2-S deposition in winter was higher than that in summer. The annual average (2008–2011) was 1.37 kg S ha^{-1} yr^{-1} for total SO_4-S deposition from MLM/wet and 8.51 kg S ha^{-1} yr^{-1} from IER throughfall measurement. The dry deposition percentage was 60% of total SO_4-S deposition according to MLM/wet mean. Total SO_4-S deposition fluxes from IER throughfall samples were higher than those from IER/wet ($p = 0.007$). The correlation coefficient was 0.75 ($p = 0.04$) indicating SO_4-S deposition from two methods tend to increase together. Based on the intercomparison of MLM and BLM, Schwede et al. (2011) concluded that the V_d of SO_2 from MLM and BLM were uncorrelated and the

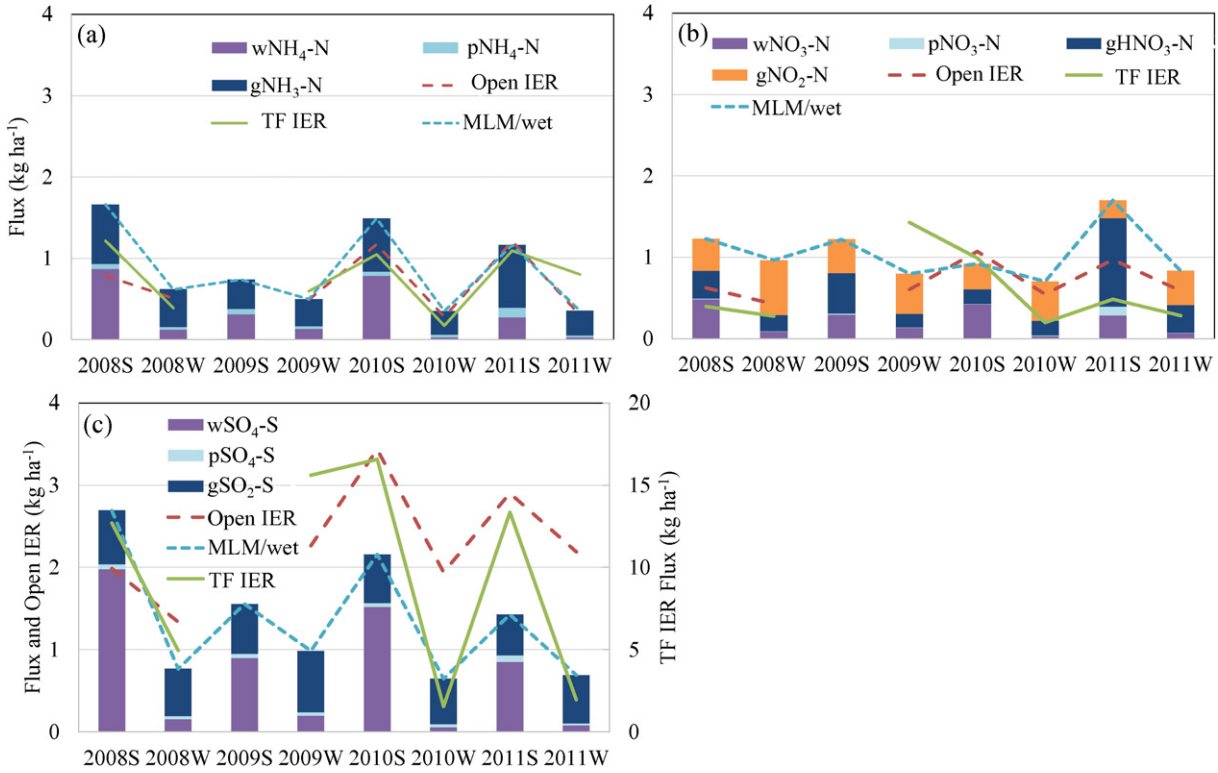

Fig. 5. Deposition flux (kg ha^{-1}) comparison for MLM/wet precipitation (dry plus wet) with open-site and throughfall IER measurements from 2008 summer to 2011 winter at AMS 1: (a) NH_4-N; (b) NO_3-N; (c) SO_4-S. (For x-axis, S is summer, from May to October; W is winter, from November to April. For legend, w is wet precipitation; p is particulate phase; g is gaseous phase; TF IER: throughfall ion exchange resin sample).

median V_d of SO_2 from MLM was 49% lower than that from BLM. Sickles and Shadwick (2007a) applied MLM to estimate S and N deposition in the eastern U.S. and also found that the V_d of SO_2 might be underestimated for forested canopies (Finkelstein et al., 2000). It is also possible that the MLM underestimated the SO_2 as S dry deposition for the near source calculation due to the rapid concentration changes.

Overall, the deposition estimates from the MLM/wet precipitation and IER throughfall measurements are in good agreement for NH_4-N and NO_3-N deposition ($p > 0.05$) and the total SO_4-S deposition from MLM/wet precipitation was much lower than that from IER throughfall. Likewise, CALPUFF model simulations for deposition of NO_3-N were in good agreement with IER NO_3-N throughfall flux data (Fenn et al., 2015). Although lower than throughfall S deposition measurements, S deposition fluxes in the region near AMS 1 based on the CALPUFF model (Davies, 2012) are approximately 4–5 kg S ha^{-1} yr^{-1}, higher than that of the MLM estimates for AMS 1 (~2.20–3.46 kg S ha^{-1} yr^{-1}; Fig. 5c). In contrast, throughfall flux measurements of S deposition at AMS 1 ranged from 15–18 kg S ha^{-1} yr^{-1} from 2008–2012 (Fenn et al., 2015). Thus it appears that neither CALPUFF nor MLM fully capture S deposition in the AOSR, but MLM in particular underestimates total inorganic S deposition. As mentioned above, this is likely at least partially due to underestimates of SO_2-S deposition, but particulate S deposition is also thought to be considerably underestimated by MLM and CALPUFF. During some upset episodes, high levels of particulate sulfate and SO_2 which reacts with NH_3 to form ammonium sulfate in the atmosphere, could be released from stacks in the AOSR. Emissions rates and forms can vary widely depending on feedstocks, petrochemicals and processes implemented (Fenn et al., 2015; Wang et al., 2012; Watson et al., 2011). For example, there was a surprising increase in throughfall SO_4-S deposition (annual throughfall deposition > 35 kg S ha^{-1}) observed and sustained for several years at a moderately-polluted site in the AOSR immediately after a dirt road was constructed and forest clearing occurred near the monitoring site (M.E. Fenn, unpublished data). This presumably resulted in high levels of dust with accumulated particulate SO_4^{2-} that had deposited to the surface soils. It is thought that SO_4^{2-} in re-suspended dust subsequently accumulated on tree canopies and was collected in throughfall samples during precipitation and snow melt events. Source apportionment studies in the AOSR have demonstrated that fugitive dust from tailing sands and haul roads, such as that mentioned above, could be a major pollutant source in the AOSR (Landis et al., 2012). Further investigation should be conducted to learn the factors resulting in the S deposition underestimation by applying MLM/wet, and improve the existing deposition models for S or to apply other means for S deposition calculations.

For terrestrial effects, analysis of soil and foliar chemistry in the AOSR (Maynard, 2015) concluded that there was no correlation between soil pH and the deposition of N and S. This is because of the co-deposition of base cations which neutralize the acid inputs (Fenn et al., 2015; Watmough et al., 2014). The elevated levels of N, S and base cations deposition in the center of the AOSR shown in Fig. 4, near emission sources, may play an important role for the ecosystem (e.g., increased cover and richness of vascular plants, a shift in species composition with the possible reduction in mosses and stress effects on lichens) as a fertilization effect of atmospheric deposition (Macdonald, 2015; Puckett, 2015).

4. Conclusions

1. The highest NO_2 and SO_2 deposition occurred near major industrial operation areas and in Fort McMurray. Concentrations in winter were much higher than those in summer. However, concentrations of NH_3 and HNO_3 were higher in the summer months, and were also enhanced outside of the mining and upgrading area, mainly in the southern portion of the study area.

2. Increased levels of NH_3 were possibly also caused by forest fires and agricultural activities in central Alberta. Nitric acid, as the secondary pollutant produced via photochemical reactions, was found far away from the center of NO_x emissions, both in the northern and southern

directions. Consequently, deposition of these pollutants as well as deposition of total gaseous inorganic N was also elevated in those areas.

3. Wet deposition of NH_4-N plus dry deposition of NH_4-N derived with MLM using passive sampler NH_3 concentration data compared well with throughfall deposition fluxes from IER samplers. Both approaches showed similar spatial patterns, and with deposition higher in summer than winter. Values for the total NO_3-N deposition from the MLM dry deposition plus wet deposition were within the same range as the IER throughfall measurements. However, wet plus dry deposition of SO_4-S was much lower than that from IER throughfall measurements. Further study should be carried out for better modeling estimates of SO_2 and SO_4^{2-} dry deposition fluxes.

4. It should be noted that these measurements do not capture all N deposition since the contribution of organic gaseous nitrogen species, HONO and NO are not included in the modeled estimates of N deposition. Future work on quantifying the contribution of these N sources towards total N deposition should be conducted for more accurate N deposition estimates.

Acknowledgements

The authors thank WBEA for providing funding in support of this work. The content and opinions expressed by the authors in this study do not necessarily reflect the views of the WBEA or of the WBEA membership. The authors would also like to thank Kristofer Siriunas for creating isopleth maps and Thomas Clair, David Spink, Sunny Cho, and Carla Davidson for their valuable comments and suggestions.

Appendix A. Supplementary data

Supplementary data to this article can be found online at http://dx.doi.org/10.1016/j.scitotenv.2016.05.205.

References

Adon, M., Galy-Lacaux, C., Delon, C., Yoboue, V., Solmon, F., Tchuente, A.T.K., 2013. Dry deposition of nitrogen compounds (NO_2, HNO_3, NH_3), sulfur dioxide and ozone in west and central African ecosystems using the inferential method. Atmos. Chem. Phys. 13, 11351–11374.

Aherne, J., Shaw, P.D., 2010. Impacts of sulphur and nitrogen deposition in western Canada. J. Limnol. 69, 1–3.

Alberta Energy, 2011. http://www.energy.gov.ab.ca/OilSands/791.asp#Geography. June 5, 2011.

Brook, J.R., Zhang, L.M., Li, Y.F., Johnson, D., 1999. Description and evaluation of a model of deposition velocities for routine estimates of air pollutant dry deposition over North America. Part II: review of past measurements and model results. Atmos. Environ. 33, 5053–5070.

Butler, T.J., Likens, G.E., 1995. A direct comparison of throughfall plus stemflow to estimates of dry and Total deposition for sulfur and nitrogen. Atmos. Environ. 29, 1253–1265.

Bytnerowicz, A., Fenn, M.E., 1996. Nitrogen deposition in California forests: areview. Environ. Pollut. 92, 127–146.

Bytnerowicz, A., Fenn, M., Allen, E., Cisneros, R., 2014. Ecologically relevant air chemistry. In: Mooney, H., Zavaleta, E. (Eds.), Ecosystems of California: A Source Book. University of California Press (in print).

Bytnerowicz, A., Fraczek, W., Schilling, S., Alexander, D., 2010. Spatial and Temporal distribution of ambient nitric acid and ammonia in the Athabasca Oil Sands Region, Alberta. J. Limnol. 69 (Suppl.), 11–21.

Bytnerowicz, A., Hsu, Y.-M., Percy, K., Legge, A., Fenn, M., Schilling, S., et al., 2016. Ground-level air pollution changes during a boreal wildland mega-fire. Sci. Total Environ. (submitted).

Bytnerowicz, A., Sanz, M.J., Arbaugh, M.J., Padgett, P.E., Jones, D.P., Davila, A., 2005. Passive sampler for monitoring ambient nitric acid (HNO_3) and nitrous acid (HNO_2) concentrations. Atmos. Environ. 39, 2655–2660.

Cooter, E.J., Schwede, D.B., 2000. Sensitivity of the National Oceanic and Atmospheric Administration multilayer model to instrument error and parameterization uncertainty. J. Geophys. Res.-Atmos. 105, 6695–6707.

Davies, M.J.E., 2012. Air quality modeling in the Athabasca Oil Sands Region. In: Percy, K.E. (Ed.), Alberta Oil Sands: Energy, Industry and the Environment. Elsevier, pp. 267–309.

Fenn, M.E., Poth, M.A., 2004. Atmospheric pollutants and trace gases: monitoring nitrogen deposition in throughfall using ion exchange resin columns: afield test in the San Bernardino Mountains. J. Environ. Qual. 33, 2007–2014.

Fenn, M.E., Bytnerowicz, A., Schilling, S.L., Ross, C.S., 2015. Atmospheric deposition of nitrogen, sulfur and base cations in jack pine stands in the Athabasca Oil Sands Region, Alberta, Canada. Environ. Pollut. 196, 497–510.

Fenn, M.E., Ross, C.S., Schilling, S.L., Baccus, W.D., Larrabee, M.A., Lofgren, R.A., 2013. Atmospheric deposition of nitrogen and sulfur and preferential canopy consumption of nitrate in forests of the Pacific northwest, USA. For. Ecol. Manag. 302, 240–253.

Finkelstein, P.L., Ellestad, T.G., Clarke, J.F., Meyers, T.P., Schwede, D.B., Hebert, E.O., et al., 2000. Ozone and sulfur dioxide dry deposition to forests: observations and model evaluation. J. Geophys. Res.-Atmos. 105, 15365–15377.

Finlayson-Pitts, B.J., Pitts, J.N., 2000. Chemistry of the Upper and Lower Atmosphere Theory, Experiments, and Applications. Academic Press, San Diego pp. xxii, 969 p.

Fowler, D., Cape, J.N., Unsworth, M.H., 1989. Deposition of atmospheric pollutants on forests. Philos. Trans. R. Soc. London, Ser. B 324, 247–265.

Hanson, P.J., Lindberg, S.E., 1991. Dry deposition of reactive nitrogen-compounds - a review of leaf, canopy and non-foliar measurements. Atmos. Environ. Part A 25, 1615–1634.

Hsu, Y.-M., 2013. Trends in passively-measured ozone, nitrogen dioxide and sulfur dioxide concentrations in the Athabasca Oil Sands region of Alberta, Canada. Aerosol Air Qual. Res. 13, 1448–1463.

Hsu, Y.-M., Bytnerowicz, A., 2015. Air pollution and dry deposition of nitrogen and sulphur in the AOSR estimated using passive samplers. In: Clair, T.A., Percy, K.E. (Eds.), Assessing Forest Health in the Athabasca Oil Sands Region. Wood Buffalo Environmental Association, Fort McMurray, Alberta, pp. 8–39.

Hsu, Y.M., Clair, T.A., 2015. Measurement of fine particulate matter water-soluble inorganic species and precursor gases in the Alberta Oil Sands Region using an improved semicontinuous monitor. J. Air Waste Manage. Assoc. 65, 423–435.

Kalberer, M., Ammann, M., Arens, F., Gaggeler, H.W., Baltensperger, U., 1999. Heterogeneous formation of nitrous acid (HONO) on soot aerosol particles. J. Geophys. Res.-Atmos. 104, 13825–13832.

Koutrakis, P., Sioutas, C., Ferguson, S.T., Wolfson, J.M., Mulik, J.D., Burton, R.M., 1993. Development and evaluation of a glass honeycomb denuder filter pack system to collect atmospheric gases and particles. Environ. Sci. Technol. 27, 2497–2501.

Krupa, S.V., 2003. Effects of atmospheric ammonia (NH_3) on terrestrial vegetation: areview. Environ. Pollut. 124, 179–221.

Krupa, S.V., Legge, A.H., 2000. Passive sampling of ambient, gaseous air pollutants: an assessment from an ecological perspective. Environ. Pollut. 107, 31–45.

Landis, M.S., Pancras, J.P., Graney, J.R., Stevens, R.K., Percy, K.E., Krupa, S., 2012. Receptor modeling of epiphytic lichens to elucidate the sources and spatial distribution of inorganic air pollution in the Athabasca Oil Sands Region. In: Percy, K.E. (Ed.), Alberta Oil Sands: Energy, Industry and the Environment. Elsevier, pp. 427–467.

Lindberg, S.E., Lovett, G.M., 1992. Deposition and forest canopy interactions of airborne sulfur - results from the integrated forest study. Atmos. Environ. Part A 26, 1477–1492.

Lovett, G.M., Lindberg, S.E., 1993. Atmospheric deposition and canopy interactions of nitrogen in forests. Can. J. For. Res. 23, 1603–1616.

Macdonald E. Responses of understory vegetation to deposition from oil sand processing operations in: Clair, TA, Percy, KE, editors. Assessing Forest Health in the Athabasca Oil Sands Region. Wood Buffalo Environmental Association, Fort McMurray, Alberta, 2015, pp. 134–144.

Maynard, D.G., 2015. Routine foliar and soil analysis of 15 years monitoring in the AOSR. In: Clair, T.A., Percy, K.E. (Eds.), Assessing Forest Health in the Athabasca Oil Sands Region. Wood Buffalo Environmental Association, Fort McMurray, Alberta, pp. 111–133.

Meyers, T.P., Finkelstein, P., Clarke, J., Ellestad, T.G., Sims, P.F., 1998. A multilayer model for inferring dry deposition using standard meteorological measurements. J. Geophys. Res.-Atmos. 103, 22645–22661.

Percy, K.E., 2013. Ambient air quality and linkage to ecosystems in the Athabasca Oil Sands, Alberta. Geosci. Can. 40, 182–201.

Percy, K.E., Hansen, M.C., Dann, T., 2012. Air quality in the Athabasca Oil Sands Region 2011. In: Percy, K.E. (Ed.), Alberta Oil Sands: Energy, Industry and the Environment. Elsevier, pp. 47–92.

Puckett, K., 2015. Chemical composition and lichen community change in the AOSR. In: Clair, T.A., Percy, K.E. (Eds.), Assessing Forest Health in the Athabasca Oil Sands Region. Wood Buffalo Environmental Association, Fort McMurray, Alberta, pp. 145–166.

Roadman, M.J., Scudlark, J.R., Meisinger, J.J., Ullman, W.J., 2003. Validation of Ogawa passive samplers for the determination of gaseous ammonia concentrations in agricultural settings. Atmos. Environ. 37, 2317–2325.

Schwede, D., Zhang, L.M., Vet, R., Lear, G., 2011. An intercomparison of the deposition models used in the CASTNET and CAPMoN networks. Atmos. Environ. 45, 1337–1346.

Seinfeld, J.H., Pandis, S.N., 2006. Atmospheric Chemistry and Physics: From Air Pollution to Climate Change. J. Wiley, Hoboken, N.J.

Sickles, J., Shadwick, D.S., 2007a. Changes in air quality and atmospheric deposition in the eastern United States: 1990–2004. J. Geophys. Res.-Atmos. 112. http://dx.doi.org/10.1029/2006JD007843.

Sickles, J.E., Shadwick, D.S., 2007b. Seasonal and regional air quality and atmospheric deposition in the eastern United States. J. Geophys. Res.-Atmos. 112. http://dx.doi.org/10.1029/2006JD008356.

Tang, H.M., Brassard, B., Brassard, R., Peake, E., 1997. A new passive sampling system for monitoring SO_2 in the atmosphere. Field Anal. Chem. Technol. 1, 307–314.

Tang, H., Lau, T., Brassard, B., Cool, W., 1999. A new all-season passive sampling system for monitoring NO_2 in air. Field Anal. Chem. Technol. 3, 338–345.

Wang, X.L., Watson, J.G., Chow, J.C., Kohl, S.D., Chen, L.-W.A., Sodeman, D.A., et al., 2012. Measurement of real-world stack emissions with a dilution sampling system. In:

Percy, K.E. (Ed.), Alberta Oil Sands: Energy, Industry and the Environment. Elsevier, pp. 171–192.
Watmough, S.A., Whitfield, C.J., Fenn, M.E., 2014. The importance of atmospheric base cation deposition for preventing soil acidification in the Athabasca Oil Sands Region of Canada. Sci. Total Environ. 493, 1–11.
Watson, J.G., Chow, J.C., Wang, X., Kohl, S.D., Gronstal, S., Zielinska, B., 2011. Winter Stack Emissions Measured With a Dilution Sampling System. Wood Buffalo Environmental Association, Fort McMurray, AB Canadawww.wbea.org.
Wesely, M.L., Hicks, B.B., 2000. A review of the current status of knowledge on dry deposition. Atmos. Environ. 34, 2261–2282.
Zhang, L., Vet, R., O'Brien, J.M., Mihele, C., Liang, Z., Wiebe, A., 2009. Dry deposition of individual nitrogen species at eight Canadian rural sites. J. Geophys. Res.-Atmos. 114. http://dx.doi.org/10.1029/2008JD010640.